Global NEST Journal, Vol 27, No X, pp 1-11

Biosorption of Basic Red 18 dye by *Aspergillus westerdijkiae* ATCC 3174 and *Aspergillus ochraceus*: optimization, kinetics, and thermodynamic studies

Hadj Daoud Bouras[1,2]*, Pinar Belibagli[3], Noureddine Bouras[2,4] and Nadir Dizge[5]**

[1]Département de l'enseignement des Sciences et des Technologies, Faculté des Sciences et de la Technologie, Université de Ghardaia, Ghardaia, Algeria.

[2]Laboratoire de Valorisation et Conservation des Ecosystèmes Arides (LVCEA), Université de Ghardaia, Ghardaia, Algeria.

[3]Department of Energy Systems Engineering, Tarsus University, Tarsus, 33400, Turkey

[4]Laboratoire de Biologie des Systèmes Microbiens (LBSM), Ecole Normale Supérieure de Kouba, BP 92, 16308, Vieux-Kouba, Alger, Algeria

[5]Department of Environmental Engineering, Mersin University, Mersin, 33343, Turkey

Received: 25/06/2025, Accepted: 02/11/2025, Available online: 10/11/2025

*to whom all correspondence should be addressed: e-mail: hadjdaoud_bouras@yahoo.fr; nadirdizge@gmail.com

https://doi.org/10.30955/gnj.07787

Graphical abstract

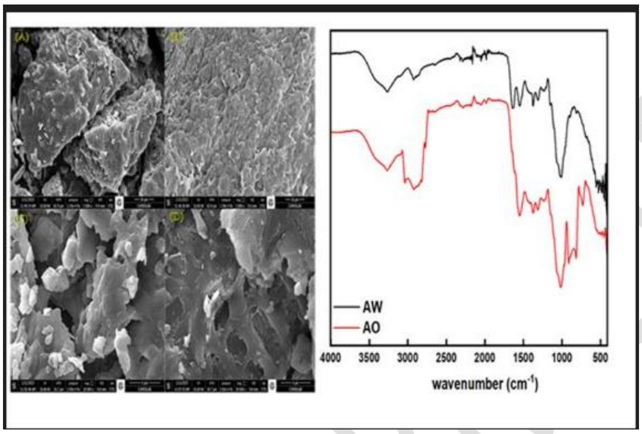

Abstract

This investigation assessed the adsorption capacities of *Aspergillus westerdijkiae* ATCC 3174 (AW) and *Aspergillus ochraceus* (AO) for Basic Red 18 (BR18). Characterization was performed using Scanning Electron Microscopy (SEM) and Fourier Transformer Infrared Spectroscopy (FTIR) techniques. Optimal sorption conditions were identified by adjusting various factors. The biosorption data were analyzed using various isotherm models. The biosorption data were analyzed, and the Langmuir model showed superior fitting to the sorption data for AO based on R^2 values, while the Temkin model provided a better fit for AW. The biosorption processes followed pseudo-second-order rate kinetics. The maximum biosorption capacity was found to be 11.95 mg/g for AW and 73.53 mg/g for AO. Thermodynamic variables related to biosorption were assessed, indicating that the dye uptake by *Aspergillus westerdijkiae* and *Aspergillus ochraceus* occurred spontaneously and was exothermic.

Keywords: *Aspergillus westerdijkiae* ATCC 3174; *Aspergillus ochraceus*; Basic Red 18; Biosorption; Kinetics; Thermodynamic study.

1. Introduction

The textile sector consumes vast amounts of water and is a key contributor to environmental contamination, discharging a wide range of harmful chemicals and persistent substances into ecosystems (Rápó *et al*. 2020; Gayathiri *et al*. 2022; El Amri *et al*. 2022). Managing these persistent organic and inorganic compounds in dye wastewater is a considerable challenge for wastewater treatment processes (Baing *et al*. 2020). Dyes pose a major environmental threat due to their resistance to natural degradation, leading to lasting ecological concerns (Samuel *et al*. 2023). The problem is worsened by the use of heavy metals like chromium and copper in textile processing, making wastewater treatment more complex (Tran *et al*. 2024). Large-scale dye production further amplifies the issue, with reactive dyes being particularly harmful due to their widespread use and high solubility, which affect aquatic life (Dutta *et al*. 2021). A significant portion of these dyes does not bind to fabrics and ends up in wastewater, disrupting photosynthesis in aquatic plants and harming organisms. Some dyes have also been associated with human health risks, including skin irritation and potential carcinogenic effects (Sudarshan *et al*. 2022). To address these challenges, improved wastewater treatment technologies are needed to ensure the safe reuse of industrial effluents, especially for irrigation (Tokay Yılmaz *et al*. 2023; Rybczyńska-Tkaczyk *et al*. 2020). Various methods have been developed to eliminate dyes, including irradiation, precipitation, and ozonation (Bouras *et al*. 2021; Singh *et al*. 2022; Batana *et al*. 2022; Yadav and Dindorkar 2022; Samiyammal *et al*. 2022). However, each of these approaches has its drawbacks—ozonation, while effective, demands significant energy input and comes with high costs, whereas membrane filtration can successfully remove dyes but tends to be maintenance-heavy and expensive to operate (Wen *et al*. 2024; Sravan *et al*. 2024). The choice of treatment method depends on multiple factors, including financial feasibility, practical applicability, and overall effectiveness in meeting purification goals (Al-Tohamy *et al*. 2022). Recent advances in wastewater recycling have demonstrated that the integration of intelligent monitoring systems can significantly enhance the security and reliability of treatment operations. For example, Selvanarayanan *et al*. (2024) developed a fuzzy logic model embedded with a recurrent neutral network (RNN) and IoT architecture to ensure secure data transmission and sustainable wastewater management in coffee farming. Similarity, Maruthai *et al*. (2025) proposed an innovative approach for wastewater recycling that integrates IoT-based sensor vision with a hybrid gated recurrent neutral networks (HG-RNN) model to enable real-time monitoring and transformation of polluted ponds into clean water systems, thereby enhancing both the reliability and security of the treatment process. Lekhya *et al*. (2025) also applied RNN and natural language processing (NLP) models to optimize water reuse, highlighting improved system dependability. Biological treatment stands out as an environmentally friendly and economically viable alternative (Shabir *et al*. 2022). Recent studies emphasize its potential, leveraging natural mechanisms to either degrade or capture dye pollutants with minimal ecological disturbance. In this regard, researchers have examined microorganisms that can neutralize or break down industrial dyes (Li *et al*. 2022; Kapoor *et al*. 2021; Mishra *et al*. 2021). Certain fungi and bacteria have demonstrated remarkable efficiency—fungal cell walls contain components that naturally bind to dye particles (Torres-Farradá *et al*. 2024), while bacterial communities secrete enzymes like laccases and peroxidases, which can dismantle complex dye structures (Karnwal 2024). Both living and non-living fungal biomass have been explored for their ability to absorb dyes, offering a sustainable and low-cost solution for wastewater treatment (Hamed and Idrus 2023; Bouras *et al*. 2019). Fungal biosorption plays a dual role in wastewater treatment by not only extracting dyes but also lowering chemical and biological oxygen demand, thereby improving water quality (Mian *et al*. 2024). Various fungal strains, including those from the *Penicillium*, *Pleurotus*, *Candida*, *Aspergillus*, and *Rhizopus* genera, have shown significant potential in breaking down dye pollutants (Danial and Dardir 2023). These fungi can adapt to diverse environmental conditions and transform complex dye compounds into less harmful byproducts, making them promising candidates for large-scale wastewater treatment (Rai and Vijayakumar 2023; Kalia *et al*. 2024). Despite these advances, the persistent contamination of water bodies indicates a continued need to identify and optimize robust fungal strains capable of efficient dye removal under varying environmental conditions. This constitutes the primary motivation for the present study, which aims to explore the biosorptive potential of dried fungal biomass as a low-cost, sustainable, and efficient solution for treating dye-contaminated wastewater.

Despite extensive research on biological dye removal, there remains lack of comparative studies examining the biosorption mechanisms and efficiency less-explored fungal species such as *Aspergillus westerdijkiae and Aspergillus ochraceus.* Furthermore, the adsorption behavior of this strains toward azo dyes, particularly Basic Red (BR 18), has not been documented. Therefore, this study aims to fill this gap by providing a comprehensive evaluation of the biosorptive performance of *A. westerdijkiae and A. ochraceus* for BR18 removal from aqueous media. The originality of this work lies in (i) the first use of these fungal strains as biosorbents for BR18, (ii) the integrated assessment of kinetic, equilibrium, thermodynamic parameters to elucidate the biosorption mechanism, and (iii) the demonstration of an eco-sustainable, low cost alternative for industrial dye wastewater treatment. These contributions are expected to expand the current understanding of fungal based biosorption and guide future applications in sustainable wastewater management.

2. Materials and Methods

2.1. Fungal strains and growth conditions

The fungi *Aspergillus westerdijkiae* ATCC 3174 (AW) and *Aspergillus ochraceus* (AO) were retrieved from a preserved strain repository. Their growth was maintained in a liquid medium, prepared according to the procedure detailed by (Bouras *et al*. 2017).

2.2. Adsorbate

The solid form of the dye under investigation, BR 18, was acquired from Dyestar (Turkey). BR 18, depicted in (**Figure 1**), exhibits cationic properties, featuring the chemical formula $C_{19}H_{25}ClN_5O_2$, a molar mass of 390.89 g/mol, and an absorption peak at 484 nm (Isik *et al*. 2023).

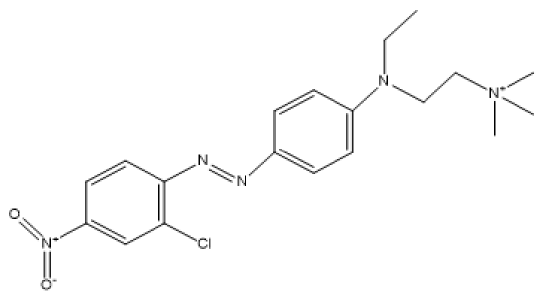

Figure 1. Chemical structure of BR18.

Stock solutions of the dye were prepared for the experiments. Working solutions were then made, and the maximum absorption wavelength (λ_{max}) for these dye solutions was measured using a T90+ UV/Vis Spectrometer (PG Instruments Ltd.).

2.3. Batch experiment procedure

Batch biosorption experiments were systematically conducted to assess how various factors influence the sorption behavior of BR 18. These factors included pH levels from 2 to 10, biosorbent dosages, initial dye concentrations, contact times, and temperatures between 298 K and 308 K. A constant pH of 10 was maintained throughout. *Aspergillus westerdijkiae* ATCC 3174 (AW) and *Aspergillus ochraceus* (AO) were added to 250 mL Erlenmeyer flasks with dye solution and mixed on a mechanical shaker at 250 rpm until equilibrium. After the designated contact time, the mixtures were centrifuged, and the remaining dye concentration was measured using a UV-Vis spectrophotometer calibrated at 484 nm. The equilibrium adsorption capacities q_e (mg/g) at different solute of concentrations of BR18 adsorbed by AW and AO were calculated according to Eq. (1).

$$q_e = \frac{(C_0 - C_e)V}{m} \qquad (1)$$

The percentage of dye biosorption (%) can be detemmined using Eq. (2):

$$\text{Biosorption percentage } \% = \frac{(C_0 - C_e)}{C_0} \times 100 \qquad (2)$$

Where C_0 and C_e are the initial and equilibrium concentrations of BR18, respectively (mg/L). V is the volume of BR18 solution (L) and m is the mass of adsorbent used (g).

2.4. Characterization of the biosorbent

The biomass was subjected to comprehensive characterization through the utilization of advanced techniques such as Scanning Electron Microscopy (SEM), specifically employing the (Zeiss Supra 55 model), FTIR and Zeta potential both prior to and following the adsorption of BR 18 dye.

3. Results and discussion

3.1. Characterization A. westerdijkiae and A. ochraceus surfaces

Scanning Electron Microscopy (SEM) is a crucial technique for examining the surface morphology of biosorbents (De Castro *et al*. 2021).

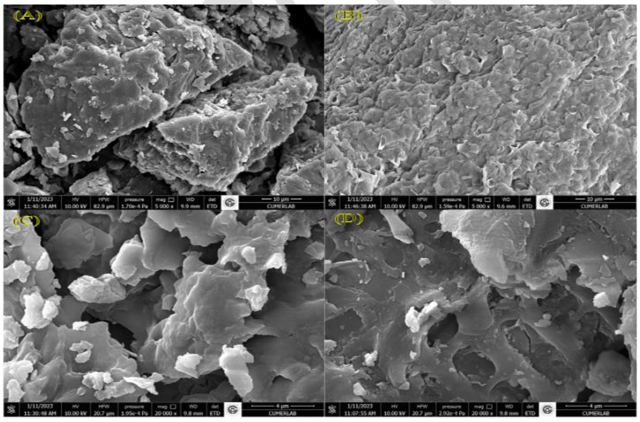

Figure 2. SEM images of (A) AW, (B) BR 18-loaded AW, (C) AO and (D) BR 18-loaded AO.

In **Figures 2 (A, B) and Figures 2 (C, D)**, the SEM images illustrate the structural features of both AW and AO, captured before and after the biosorption process. These micrographs highlight the presence of irregular pores on the surfaces of AW and AO, providing suitable sites for the entrapment and adsorption of dye molecules (**Figure 2A**) and (**Figure 2C**). After BR 18 adsorption, a noticeable change occurs, with the surfaces of both AW and AO being uniformly coated with the dye, indicating successful adsorption of BR 18 onto the biosorbents (**Figure 2B**) and (**Figure 2D**) (Munagapati *et al*. 2022). The zeta potential measurements of the fungal biosorbents AW and AO were conducted over a pH range of 2 to 10 to evaluate the surface charge behavior and its influence on BR18 dye adsorption.

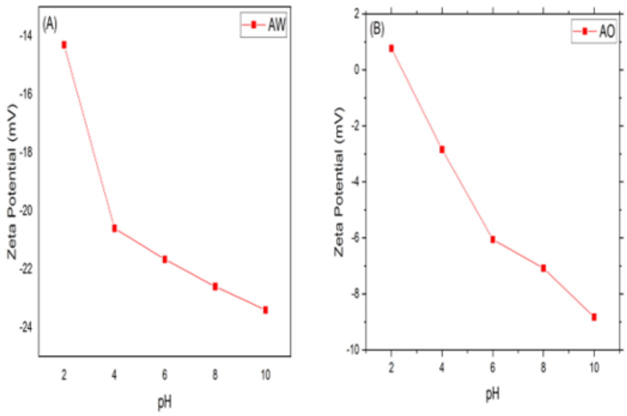

Figure 3. Zeta potential results of (A) *Aspergillus westerdijkiae* and (B) *Aspergillus ochraceus* fungal

As shown in **Figure 3.**, both biosorbents exhibited negative zeta potential values that became increasingly negative with rising pH, indicating the deprotonation of surface functional groups such as carboxyl and hydroxyl moieties. For AO, the zeta potential shifted from a slightly positive value of +0.77 mV at pH 2 to a negative value of -8.82 mV at pH 10, suggesting that its surface is weakly charged and that the isoelectric point lies close to acidic conditions. In contrast, AW displayed more negative values across the entire pH range, varying from -14.31 mV at pH 2 to -23.4 mV at pH 10. The higher magnitude of negative charge observed for AW implies a greater abundance of ionizable acidic groups and a stronger electrostatic affinity toward the cationic BR18 molecules. These findings indicate that AW processes a more stable and negatively charged surface compared to AO, witch can enhance electrostatic attraction and dye adsorption capacity.

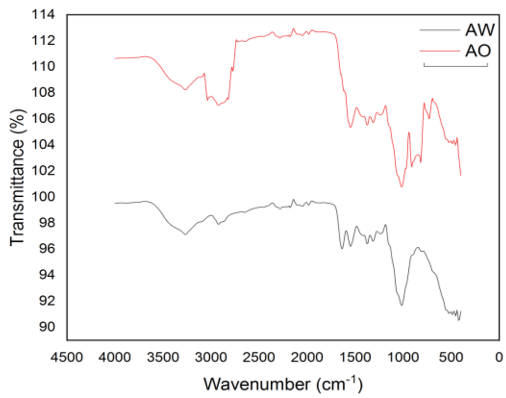

Figure 4. FTIR spectrum of AW and AO biosorption.

Figure 4 presents the FTIR spectra of AW and AO after the biosorption process, revealing similar structural features for both fungi. The peak observed at 3165 cm^{-1} is associated with the overlapping of –OH and –NH groups, while the peak at 2930 cm^{-1} corresponds to C–H stretching. The signal at 1555 cm^{-1} indicates the presence of an amide group, likely from proteins. Other peaks found at 1625, 1386, 647, 553, and 481 cm^{-1} are linked to N–H bending, $–CH_3$ wagging, O–C–O scissoring, C–O bending, and C-N-C stretching vibrations, respectively, highlighting the presence of multiple functional groups. Similar FTIR patterns have been observed for dye compounds on various fungal biomasses (Arslantaş *et al*. 2022; Bayramoğlu and Arıca 2008; Hasani *et al*. 2017).

3.2. Effect of pH on biosorption

The pH level of the biosorption medium plays a pivotal role in influencing the uptake of dye from aqueous solutions by biosorbents. In light of this, the adsorption of BR 18 dye onto both AW and AO was meticulously examined. For these investigations, 1 g/L of biosorbent was employed, and the initial dye concentration was set at 10 mg/L, with pH values ranging from 2 to 10 being considered. The findings, as illustrated in **Figure 5**, unveil distinct patterns: AW exhibits its maximum biosorption capacity at pH 10, reaching an impressive 82.31±4.5%, while AO's peak performance is observed at pH 8, with an uptake rate of 67.74±3.8%. These outcomes strongly suggest that the biosorption of BR 18 onto both fungi is most favorable under alkaline conditions. It's plausible that under these alkaline conditions, the biosorbent's surface develops a more pronounced negative charge as the initial solution pH rises, thereby enhancing the attraction of dye cations via electrostatic forces. Conversely, the lowest removal percentages observed at acidic pH levels result from repulsive forces between the biosorbent surface and the cationic dye. Comparable findings have been documented in previous studies involving materials like *Tectona grandis* sawdust and brewers' spent grain (Mashkoor *et al*. 2018; Chanzu *et al*. 2019).

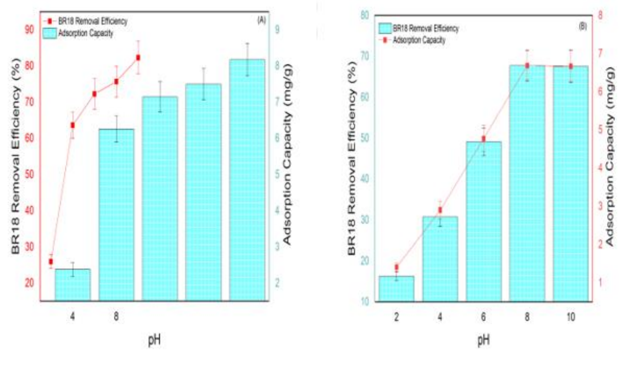

Figure 5. Effect of pH on the biosorption capacity of BR 18 on *A. westerdijkiae* and *A. ochraceus*.

3.3. Effect of adsorbent dose

Figure 6 shows the effect of adsorbent dose on BR18 removal efficiency. According to the results for AW fungus, the minimum BR18 removal efficiency was 72.1±0.41% with 0.5 g/L AW adsorbent dose. It is seen that the removal efficiency remains constant as the adsorbent dose increases. This result can be explained by the adsorbent reaching the saturation point. According to the results for AO fungus, the removal efficiency decreased as the adsorbent dose increased. The optimal adsorbent dosage was determined to be 1 g/L for the AW fungus, while for the AO fungus, the ideal amount was found to be 0.5 g/L.

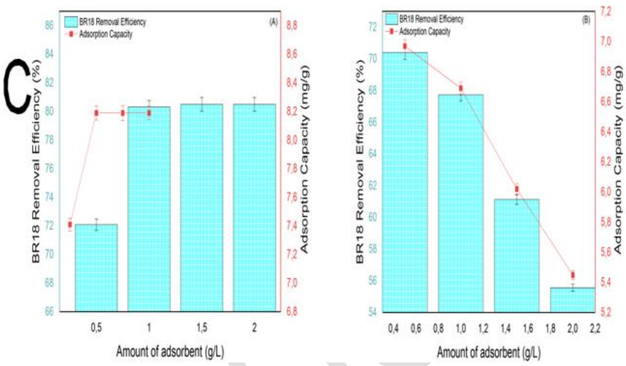

Figure 6. Effect of adsorbent amount on the biosorption capacity of BR 18 on **(A)** *A. westerdijkiae*, and **(B)** *A. ochraceus.*

3.4. Effect of contact time

The influence of contact duration, ranging from 5 to 60 minutes, on the biosorption capabilities of AW and AO at an initial dye concentration of 10 mg/L is visually presented in **Figure 7**. As depicted in the figure, the biosorption capacities exhibit a noticeable increment as the contact duration extends, ultimately reaching an equilibrium state at approximately 60 minutes for both AW and AO. At this equilibrium point, the percentage removal of BR 18 achieved by AW stood at 82.22±0.62%, compared to 69.42±0.56% for AO, given an initial BR 18 concentration of 10 mg/L. Subsequent extensions of the contact duration did not result in a further enhancement of the biosorption extent.

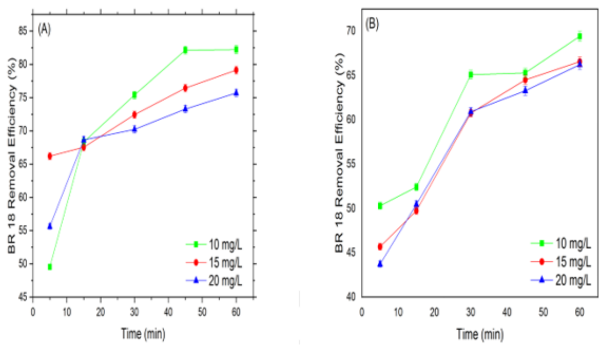

Figure 7. Impact of contact duration on BR 18's ability to biosorb on **(A)** *A. westerdijkiae* and **(B)** *A. ochraceus*

3.5. Effect of temperature on Basic Red 18 biosorption

Temperature is a key factor in practical adsorption applications. To investigate its effect on the biosorption capacity of *Aspergillus westerdijkiae* (AW) and *Aspergillus ochraceus* (AO), experiments were conducted at 298 K, 308 K, and 318 K. The optimal temperature for the biosorption of BR 18 onto *A. westerdijkiae* and *A. ochraceus* was found to be 298 K. **Figure 8** illustrates a decrease in the removal of BR 18 as temperatures rose from 298 to 308 K, indicating an exothermic nature of the sorption process. The equilibrium adsorption capacity was influenced by temperature, leading to a reduction in the percentage removal of BR 18 by AW and AO from 82.31±4.5% to 62.42±3.3%and 70.47±4.0% to 57.14±2.8% mg/g, respectively, with an increase in temperature from 298 to 308 K. This reduction may be attributed to increased movement of adsorbate molecules within the adsorbent particles (Hassan *et al*. 2020). However, temperatures exceeding 308 K may increase the flexibility of the biosorbent structure and promote the opening of internal pores in AW, leading of the exposure of additional sorption sites, and, consequently, a slightly higher adsorption rate.

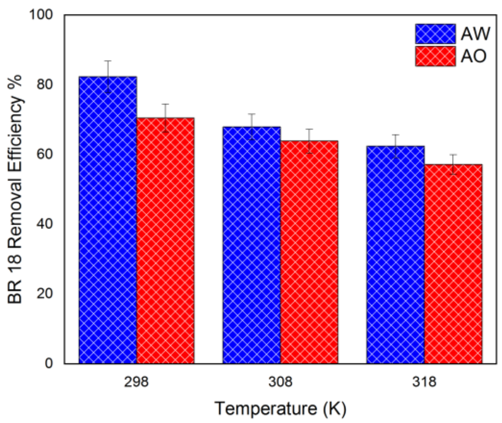

Figure 8. Impact of temperature on the biosorption capacity of BR 18 on *A. westerdijkiae* and *A. ochraceus*

3.6. Kinetic analysis of dye biosorption

The Lagergren's pseudo-first-order, pseudo-second-order, and Elovich models were applied to investigate the kinetics of biosorption of BR 18 onto AW and AO biomass. The intra-particle diffusion model was applied to investigate the rate determining step. This analysis utilized experimental data collected at various initial concentrations. The linearized form of the pseudo-first-order rate equation is represented as follows (Bouras *et al*. 2015):

$$\ln\left(q_e - q_t\right) = lnq_e - \frac{k_1}{2.303}t \quad (3)$$

Here, q_e and q_t denote the amounts of BR 18 dye sorbed at equilibrium time (mg/g) and time t (*min*), respectively, and K_1 is the first-order rate constant (min^{-1}) . The pseudo-second-order rate equation is expressed as (Koyuncu and Kul 2020):

$$\frac{t}{q_t} = \frac{1}{k_2 q_2^2} + \frac{1}{q_2}t \quad (4)$$

In this equation, k_2 (mg/g.min) is the second-order rate constant, (mg/g) is the amount of biosorption after time t (*min*), and q_e is the amount of biosorption at equilibrium (mg/g). The Elovich kinetic equation stands out as a highly applicable and fitting model for characterizing chemical adsorption. This model operates under the premise that the rate diminishes over time, attributing it to an augmentation in surface coverage in reactions involving the chemical adsorption of gases onto a solid surface, with no subsequent desorption of the products. The Elovich kinetic equation is mathematically represented by the following form (Li *et al*. 2023).

$$q_t = \frac{1}{\beta}Ln\left(\alpha\beta\right) + \frac{1}{\beta}Lnt \quad (5)$$

The mechanisms governing intraparticle diffusion phenomena evolve through a combination of compelling pore volume diffusion, surface diffusion, or a fusion of both mechanisms (Syafiuddin and Fulazzaky 2021). The initial rate of intraparticle diffusion is quantified by Eq. (6):

$$q_t = k_d t^{\frac{1}{2}} + C \quad (6)$$

Where k_d represents the intraparticle diffusion rate constant $\left(mg\cdot\left(g\cdot min^{1/2}\right)^{-1}\right)$ and C is associated with the boundary layer thickness.

The kinetic parameters for various initial dye concentrations are summarized in **Table 1**. The pseudo-first-order model yielded R^2 values slightly lower than those of the pseudo-second-order, with both showing relatively close correlation coefficients (R^2 <0.982). This small difference indicates that both kinetic models can reasonably described the biosorption behavior, particularly, at higher biosorbent doses. However, the second-pseudo-order model provided a marginally better fit, with calculated adsorption capacities closely matching the experimental data. This suggests that the biosorption of BR 18 onto *Aspergillus westerdijkiae* and *Aspergillus ochraceus* is primarily governed by chemisorption involving valence forces through the sharing or exchange of electrons between the dye molecules and active sites on the biosorbents. Comparable patterns have been reported in studies using chalcone-derived adsorbents for Basic Red 18 (Rashdan *et al*. 2023) and in recent findings where both pseudo-first-order and second-pseudo-order models exhibited close R^2 at elevated adsorbent concentrations (Dari *et al*. 2025). To assess the rate of mass transfer in the biosorption of BR 18 dye by *Aspergillus westerdijkiae* ATCC 3174 (AW) and *Aspergillus ochraceus* (AO), the intraparticle diffusion model was employed. The q_t versus $t^{0.5}$ plot (figure not shown) exhibited an intercept that did not pass through the origin, indicating that intraparticle diffusion was not the sole rate-controlling mechanism in the overall biosorption process. This observation suggests that external mass transfer and surface adsorption may also contribute to the rate limitation, particularly, due to variations in the mass transfer between the initial and equilibrium stages. Similar behavior has been documented in the biosorption of Congo Red and Acid Blue 25 onto jute stick powder and *Penicillium* YW 01 biomass, respectively (Yang *et al*. 2011). In contrast, the Elovich model did not provide a satisfactory fit to the experimental data. However, the parameters α and β derived from this model provide insight into the initial adsorption rate and biosorbent surface properties, witch may be influenced by variations in energy release during surface interactions or differences in activation energy arising from structural heterogeneity (Verma *et al*. 2017). Notably, increasing the dye concentration from 10 to 20 mg/L resulted in a higher α value and a lower β value. Furthermore, the intraparticle diffusion model, derived from the Weber and Morris framework, was employed to further analyze the adsorption mechanism of BR18 onto AW and AO.

Table 1. The comparison includes the sorption rate constants and the calculated and experimentalq_2 values for the adsorption of Basic Red 18 onto *Aspergillus westerdijkiae* and *Aspergillus ochraceus* at various initial dye concentrations.

Samples		**AW**			**AO**	
BR 18 (mg/L)	10	15	20	10	15	20
q_{eq} (exp) (mg/g)	08.43	11.78	14.91	06.90	10.33	13.74
			Pseudo-first order kinetic model			
BR 18 (mg/L)	10	15	20	10	15	20
K_1 (min^{-1})	1.33 × 10^{-2}	7.46 × 10^{-2}	9.80 × 10^{-2}	4.45 × 10^{-2}	6.02 × 10^{-2}	5.35 × 10^{-2}
q_1 (cal) (mg/g)	11.75	02.21	06.13	02.49	05.22	06.38
R^2	0.772	0.841	0.997	0.859	0.975	0.982
			Pseudo-second order kinetic model			
BR 18 (mg/L)	10	15	20	10	15	20
K_2 (g/mg.min)	2.22 × 10^{-2}	6.65 × 10^{-2}	3.25 × 10^{-2}	3.50 × 10^{-2}	2.00 × 10^{-2}	15 × 10^{-2}
q_2 (cal) (mg/g)	09.11	12.02	15.46	07.23	11.03	14.60
R^2	0.993	0.999	0.999	0.995	0.996	0.997
			Elovich kinetic model			
BR 18 (mg/L)	10	15	20	10	15	20
α (mg/g.min)	12.88	06.84	06.88	2.87	4.00	5.19
β (g/mg)	0.74	0.38	0.28	0.64	0.42	0.31
R^2	0.941	0.780	0.874	0.890	0.918	0.930
			Intraparticle diffusion kinetic model			
BR 18 (mg/L)	10	15	20	10	15	20
K_{id} (mg/g min$^{1/2}$)	0.595	0.287	0.691	0.595	0.287	0.691
C	4.139	9.725	10.168	4.139	9.725	10.168
R^2	0.903	0.874	0.834	0.903	0.874	0.834

3.7. Biosorption isotherm models

Isotherm investigations at equilibrium are crucial for gaining insights into the biosorption mechanism (Yaacoobi *et al*. 2024). The analysis of equilibrium data involved the application of well-established isotherm models, including Langmuir, Freundlich, Temkin and Dubinin–Radushkevich adsorption isotherms. The linear representation of the Langmuir model is presented as (Bouras *et al*. 2021):

$$\frac{1}{q_e} = \left(\frac{1}{K_L q_m}\right)\frac{1}{C_e} + \frac{1}{q_m} \quad (7)$$

Here, ce denotes the equilibrium concentration (mg/L), and q_e stands for the adsorbed amount at equilibrium (mg/g). The Langmuir constants, q_m (mg/g), signify the monolayer biosorption capacity, while K_L (L/mg) is associated with the heat of biosorption. The fundamental features of the Langmuir model can be articulated using a dimensionless constant termed the separation factor or equilibrium parameter, R_L. This parameter is defined as (Wang *et al*. 2020):

$$R_L = 1/\left(1 + K_L C_0\right) \quad (8)$$

Here, C_0 represents the initial concentration of the dye (mg/L). The R_L value serves as an indicator for the nature of the isotherm: irreversible ($R_L = 0$), favorable ($0 < R_L < 1$), linear ($R_L = 1$), or unfavorable ($R_L > 1$).

The Freundlich isotherm posits a surface heterogeneity characterized by a non-uniform distribution of biosorption heat across the surface (Sillanpää *et al*. 2023). This is mathematically represented by the following equation:

$$Ln\, q_e = Ln\, K_F + \left(\frac{1}{n}\right) Ln\, C_e \quad (9)$$

Here, K_F ((mg/g) (L/mg)$^{1/n}$), referred to as the adsorption or distribution coefficient, is linked to the adsorption capacity, and n represents a measure of adsorption intensity, providing insights into the favorability of the adsorption process.

The Temkin isotherm postulates that (i) the heat of adsorption for all molecules within the layer diminishes linearly with coverage, a result of interactions between adsorbent and adsorbate; and (ii) adsorption is defined by a consistent distribution of binding energies, reaching a maximum binding energy (Tukaram bai *et al*. 2020). This is mathematically represented by the following equation:

$$q_e = \frac{RT}{b_T} Ln\, C_e + \frac{RT}{b_T} Ln\, K_T \quad (10)$$

The Temkin constants, denoted as K_T (L/g) and b_T (kJ/mol), were obtained by analyzing the slopes and intercepts of plots generated from the correlation of q_e and Ln C_e.

The D–R (Dubinin–Radushkevich) isotherm equation, outlined in Equation (11) (Arslan and Kütük 2023), serves the purpose of discriminating between physical and chemical adsorption.

$$\text{Ln } q_e = -\beta\varepsilon^2 + \text{Ln } q_{DR} \quad (11)$$

Polanyi potential (ε) is given as Equation (11):

$$\varepsilon = \text{RT Ln}\left(1 + \frac{1}{C_e}\right) \quad (12)$$

The Dubinin–Radushkevich maximum adsorption capacity of the dye is represented by q_{DR} (mg/g), with β being the Dubinin–Radushkevich constant (mol²/kJ²). R denotes the universal gas constant (8.314 J/mol K), and T represents the absolute temperature (K). By plotting $\text{Ln } q_e$ against ε^2, a linear relationship emerges with a slope corresponding to β and an intercept aligning with $Ln\, q_{DR}$. The Dubinin–Radushkevich constant offers valuable insights into the mean energy of adsorption through the following equation:

$$E = \frac{1}{\sqrt{2\beta}} \quad (13)$$

Table 2 provides the parameters for the adsorption isotherms along with their corresponding fit indicators. According to the analytical findings, both the Langmuir and Freundlich models excellently characterize the biosorption isotherm data for AO, as evidenced by their high R^2 values of 0.999 and 0.997, respectively.

Table 2. details the isotherm data for the biosorption of Basic Red 18 from aqueous solutions onto *Aspergillus westerdijkiae* and *Aspergillus ochraceus*.

Sample	AW	AO
Langmuir isotherm model		
q_m (mg/g)	11.95	73.53
K_L (L/mg)	0.037	0.033
R_L	0.84-0.57	0.85-0.60
R^2	0.796	0.999
Freundlich isotherm model		
K_F (mg/g) $(mg/L)^{1/n}$	01.62	02.45
n	0.65	1.13
R^2	0.833	0.997
Temkin isotherm model		
K_T (L/g)	1.172	1.035
b_T (kJ/mole)	0.296	0.379
R^2	0.882	0.972
Dubinin-Radushkevich isotherm model		
q_{DR} (mg/g)	17.76	12.72
β (mole²/kJ²)	9E-07	9E-07
E (kJ/mole)	0.745	0.745
R^2	0.829	0.937

Table 3. Comparison of biosorption capacities of various biosorbents for removal of Basic Red18

Biosorbent	pH	q_m (mg/g)	Reference
Aspergillus ochraceus	8.00	73.53	Present work
Aspergillus westerdijkiae	10.00	11.95	Present work
Russula brevipes	6.00	21.00	Arslantaş et al. 2022
Activated sludge	7.00	285.71	Gulnaz et al. 2004
Tamarind hull	8.00	66.667	Khorramfar et al. 2010
Macroalga Caulerpa lentillifera	6.80	37.17	Marungrueng and Pavasant 2006
Bagasse pith	7.00	38.79	Slimani et al. 2014
Oreganum stalk	7.00	38.20	Toptas et al. 2014
SMC	2.00	61.72	Fil et al. 2013
Jute stick powder	4.00	530.645	Praveen et al. 2021
Rice husk based biochars	8.00	44.00	Deniz and Kepekci 2016
Spirulina platensis microalga	6.00	33.33	Sivarajasekar et al. 2017
Waste cotton seed	12.00	50.11	Deniz 2014
Cone Shell of Calabrian Pine	8.00	68.075	Senthil Rathi and Senthil Kumar 2021
Orange peel	8.20	1.37	Arjona et al. 2018

Examination of **Table 2** reveals that R_L values, falling within the typical range of 0 to 1 across all initial concentrations, indicate the favorable biosorption of BR 18 onto AW and AO within the 5–20 mg/L range. A value of n greater than unity suggests the advantageous biosorption of the dye anion by AO (Bayat *et al*. 2023).

The isotherm models suggest that the biosorbents might undergo monolayer adsorption on surfaces with diverse properties. The Temkin model results indicate that for AW and AO, the parameters are 1.172 L/g and 1.035, and 0.296 kJ/mole and 0.379, respectively. An R^2 of 0.882 confirms that the adsorption of BR 18 onto AW aligns with the Temkin isotherm, a finding that has not been documented before. The (D-R) isotherm parameter provides insights into the process. For both fungi AW and AO, the energy values were below 8 kJ/mol, suggesting that the dye's biosorption was likely governed by physical mechanisms.

3.8. Comparation

Table 3 compares the maximum adsorption capacities of AW and AO with those of various other adsorbents reported in the literature.

The results show that AW and AO demonstrate notably high adsorption capacities for Basic Red compared to many other materials. Among 13 different adsorbents, only two had a higher sorption capacity than AO (Arslantaş *et al*. 2022; Gulnaz *et al*. 2004; Khorramfar *et al*. 2010; Marungrueng and Pavasant 2006; Slimani *et al*. 2014; Toptas *et al*. 2014; Fil *et al*. 2013; Praveen *et al*. 2021; Deniz and Kepekci 2016; Sivarajasekar *et al*. 2017; Deniz 2014; Senthil Rathi and Senthil Kumar 2021; Arjona *et al*. 2018), positioning AO as moderately effective. Additionally, AW and AO are not only highly effective for BR adsorption but also offer a cost advantage over activated carbon, which is a widely used commercial adsorbent.

3.9. Thermodynamic analysis of biosorption process.

To assess the thermodynamic aspects of the dye removal process utilizing AW and AO biosorbents, we examined variations in Gibbs free energy (ΔG°), enthalpy (ΔH°), and entropy (ΔS°). Temperature-dependent equilibrium constant (K_d) was employed for this purpose. The thermodynamic parameters were estimated using the following equations.

$$\Delta G^\circ = -RT\ln K_d \tag{14}$$

$$\ln K_d = -(\Delta H^\circ)/RT + (\Delta S^\circ)/R \tag{15}$$

The ΔH° and ΔS° values were calculated using the slope and intercept of the natural logarithm of the equilibrium constant ($\ln K_d$) plotted against the reciprocal of temperature (1/T). The resulting thermodynamic data are summarized in **Table 4**. As temperature increased, the negative ΔG° values confirmed the feasibility and spontaneous nature of BR 18 dye biosorption onto both *Aspergillus westerdijkiae* ATCC 3174 (AW) and *Aspergillus ochraceus* (AO) (Arslantaş *et al*. 2022; Deniz and Kepekci 2016). The ΔH° were determined to be -40.81 kJ/mol for AW and -22.93 kJ/mol for AO, indicating that the adsorption process were exothermic within the temperature range of 298-318 K. The corresponding ΔS° values of -0.124 kJ/mol.K for AW anf -0.070 kJ/mol.K for AO reflect the decrease in randomness at the solid-liquid interface during dye uptake. The relatively low ΔS° values suggest minimal change in entropy during the adsorption process.

Table 4. Thermodynamic parameters for the biosorption of Basic Red 18 onto *A. westerdijkiae* and *A. ochraceus* at different temperatures.

Adsorbent	Temperature (K)	ΔG° (kJ/mol)	ΔH° (kJ/mol)	ΔS° (kJ/ (mol K))
AW	298	- 3.60	- 40.81	- 0.124
	308	- 2.36		
	318	-1.11		
AO	298	- 2.16	- 22. 93	- 0.070
	308	- 1.47		
	318	-0.77		

4. Conclusion

This study provides new insights into the biosorptive removal of the azo dye Basic Red 18 (BR18) using two fungal species, *Aspergillus westerdijkiae* and *Aspergillus ochraceus*. The comparative investigation revealed that *A. westerdijkiae* exhibited the highest removal efficiency (82% at 10 mg/L), highlighting its superior affinity toward BR18 under alkaline conditions. The biosorption process followed the pseudo-second order kinetic model and was well described by the Langmuir isotherm, confirming the predominance of monolayer aadsorption. Thermodynamic analysis indicated an exothemic nature of the interaction. Beyond these findings, the novelty of this work lies in demonstrating, for the first time, the potential of *Aspergillus westerdijkiae* and *Aspergillus ochraceus* as effective, eco-sustainable biosorbents for azo dye removal. The combined kinetic, equilibrium and thermodynamic approach used here contributes to better understanding of the adsorption mechanism and provides a scientific basis for scaling up fungal biosorption in wastewater treatment systems. Overall, this study not only enriches the current knowledge of fungal biosorbents but also offers promising and low-cost alternative for mitigating dye pollution in industrial effluents.

References

Al-Tohamy R., Ali S.S., Fanghua Li. F., Okasha K.M., Yehia A.-G. Mahmoud Y.A.-G., Elsamahy T., Jiao H., Fu Y. and Sun J. (2022). A critical review on the treatment of dye-containing wastewater: Ecotoxicological and health concerns of textile dyes and possible remediation approaches for environmental safety, *Ecotoxicology and Environmental Safety*, **231**, 113160. https://doi.org/10.1016/j.ecoenv.2021.113160

Arjona A., Canal J.M. and Raurich J.G. (2018). A new biosorbent with controlled grain (I). Efficient elimination of cationic dyes from textile dyeing wastewater. *International Journal of Environmental & Agriculture Research*, **4** (3), 14-27. https://doi.org/10.5281/zenodo.1213556

Arslan S. and Kütük N. (2023). Symbolic regression with feature selection of dye biosorption from an aqueous solution using pumpkin seed husk using evolutionary computation-based automatic programming methods. *Expert Systems with Applications*, **231**, 120676. https://doi.org/10.1016/j.eswa.2023.12067

Arslantaş C., M'barek I., Saleh M., Isik Z., Ozdemir S., Dundar A. and Dizge N. (2022). Basic red 18 and remazol brilliant blue R biosorption using *Russula brevipes*, *Agaricus augustus*, *Fomes fomentarius*, *Water Practice & Technology*, **17** (3), 749-762. https://doi.org/10.2166/wpt.2022.008

Karnwal A. (2024). Unveiling the promise of biosorption for heavy metal removal from water sources, Desalination and Water Treatment, 319, 100523. https://doi.org/10.1016/j.dwt.2024.100523

Baing U., Uddin M.K. and Gondal M.A. (2020). Removal of hazardous azo dye water using syhthetic nano adsorbent: Facile synthesis, characterization, adsorption, regeneration and design of experiments, *Colloids and Surfaces A: Physicochemical and Engineering Aspects*, **584**, 124031. https://doi.org/10.1016/j.colsurfa.2019.124031

Batana F.Z., Bouras H.D. and Aouissi H. (2022). Biosorption of Congo red and Basic fuchsin using micro-fungi *Fusarium oxysporum* f. sp. *Pisi* as a biosorbent: Modeling optimization and kinetics study, *Egyptian Journal of Chemistry*, **65** (13), 225-235 10.21608/EJCHEM.2022.113994.5188

Bayat M., Salehi E. and Mahdieh M. (2023). *Chromochloris zofingiensis* microalgae as a potential dye adsorbent: Adsorption thermo-kinetic, isothermal, and process optimization, *Algal Research*, **71**, 103043. https://doi.org/10.1016/j.algal.2023.10304

Bayramoğlu G. and Arıca M.Y. (2008). Removal of heavy mercury (II), cadmium (II) and zinc (II) metal ions by live and heat inactivated Lentinus edodes pellets, *Chemical Engineering Journal*, **143** (1-3), 133-140. https://doi.org/10.1016/j.cej.2008.01.002

Bouras H.D., Benturki O., Bouras N., Attou M., Donnot A., Merlin A., Addoun F. and D Holtz M. (2015). The use of an agricultural waste material from Ziziphus jujuba as a novel adsorbent for humic acid removal from aqueous solutions. *Journal of Molecular Liquids*, **211**, 1039–1046. https://doi.org/10.1016/j.molliq.2015.08.028

Bouras H.D., Isik Z., Arikan E.B., Bouras N., Chergui A., Yatmaz H.C. and Dizge N. (2019). Photocatalytic oxidation of azo dye solutions by impregnation of ZnO on fungi, *Biochemical Engineering Journal*, **146**, 150-159. https://doi.org/10.1016/j.bej.2019.03.014

Bouras H.D., Isik, Z., Arikan E.B., Yeddou A.R., Bouras N., Chergui A., Favier L., Amrane A. and Dizge N. (2021). Biosorption characteristics of methylene blue dye by two fungal biomasses. *International Journal of Environmental Studies*, **78** (3), 365-381. https://doi.org/10.1080/00207233.2020.1745573

Bouras H.D., Yeddou A.R., Bouras N., Chergui A., Favier L., Amrane A. and Dizge N. (2021). Biosorption of cationic and anionic dyes using the biomass of *Aspergillus parasiticus* CBS 100926^{T}, *Water Science and Technology*, **83** (3), 622-630 https://doi.org/10.2166/wst.2021.005

Bouras H.D., Yeddou A.R., Bouras N., Hellel D., Holtz M.D., Sabaou N., Chergui A. and Nadjemi B. (2017). Biosorption of Congo red dye by *Aspergillus carbonarius* M333 and *Penicillium glabrum* Pg1: Kinetics, equilibrium and thermodynamic studies, *Journal of the Taiwan Institute of Chemical Engineers*, **80**, 915 – 923 https://doi.org/10.1016/j.jtice.2017.08.002

Chanzu H.A., Onyari J.M. and Shiundu P.M. (2019). Brewers' spent grain in adsorption of aqueous Congo Red and malachite Green dyes: Batch and continuous flow systems, *Journal of Hazardous Materials*, **380**, 120897. https://doi:10.1016/j.jhazmat.2019.120897

Danial A.W. and Dardir F.M. (2023). Copper biosorption by *Bacillus pumilus* OQ931870 and *Bacillus subtilis* OQ931871 isolated from Wadi Nakheil, Red Sea, Egypt, *Microbial Cell Factories*, **22**, 152. https://doi.org/10.1186/s12934-023-02166-3

Dari A., Shorbaz M., Ali M. and Zamil A. (2025). Synthesis and characterization of a CNT/Fe_2O_3/ TiO_2/Bentonite nanocomposite for photocatalytic degradation of tetracycline hydrochloride, *Iranian Journal of Catalysis*, **15** (3), 152535 (1-11). https://doi.org/10.57647/j.ijc.2025.1503.35

De Castro K.C., Leme V.F.C., Souza F.H.M., Costa G.O.B., Santos G.E., Litordi L.R.V. and Andrade G.S.S. (2021). Performance of inactivated *Aspergillus oryzae* cells on dye removal in aqueous solutions, *Environmental Technology & Innovation*, **24**, 101828. https://doi.org/10.1016/j.eti.2021.101828

Deniz F. (2014). Optimization of Biosorptive Removal of Dye from Aqueous System by Cone Shell of Calabrian Pine, *The Scientific World Journal*, https://doi.org/10.1155/2014/138986

Deniz F. and Kepekci R.A. (2016). Biosorption of dye from synthetic wastewater using alga enriched in phenolic compounds, *Environmental Progress & Sustainable Energy*, **35** (3), 737–742. https://doi:10.1002/ep.12286

Dutta S., Gupta B., Srivastava S.K. and Gupta A.K. (2021). Recent advances on the removal of dyes from wastewater using various adsorbents: a critical review, *Materials Advances*, **2**, 4497 https://doi.org/10.1039/d1ma00354b

El Amri A., Bensalah J., Idrissi A., Lamya K., Ouass A., Bouzakraoui S., Zarrouk A., Rifi E. and Lebkiri A. (2022). Adsorption of a cationic dye (Methylene bleu) by *Typha Latifolia*: Equilibrium, kinetic, thermodynamic and DFT calculations, *Chemical Data Collections*, **38**, 100834. https://doi.org/10.1016/j.cdc.2022.100834

Fil B.A., Karcioglu Karakas Z., Boncukcuiglu R. and Yilmaz A.E. (2013). Removal of cationic dye (basic red 18) from aqueous solution using natural turkish clay, *Global NEST Journal*, **15** (4), 529-541. https://doi.org/10.30955/gnj.000944

Gayathiri E., Prakash P., Selvam K., Awasthi M.K., Gobinath R., Karri R.R., Ragunathan M.G., Jayanthi J., Mani V., Poudineh M.A., Chang S.W. and Ravindran B. (2022). Plant microbe based remediation approaches in dye removal: Review, *Bioengineered*, **13** (3), 7798-7828. https://doi.org/10.1080/21655979.2022.2049100

Gulnaz O., Kaya A., Matyar F. and Arikan B. (2004). Sorption of basic dyes from aqueous solution by activated sludge,

Journal of Hazardous Materials, **108** (3), 183-188. https://doi.org/10.1016/j.jhazmat.2004.02.012
Hamed H.N. and Idrus S. (2022). Adsorbents for the removal of Methylene Blue from Wastewater: A Review, *Polymers*, **14** (4), 783. https://doi.org/10.3390/polym14040783
Hasani S., Ardejani F.D. and Olya M.E. (2017). Equilibrium and kinetic studies of azo dye (Basic Red 18) adsorption onto montmorillonite: Numerical simulation and laboratory experiments, *Korean Journal of Chemical Engineering*, **34**, 2265-2274. https://doi.org/10.1007/s11814-017-0110-5
Hassan W., Noureen S., Mustaqeem M., Saleh T.A. and Zafar S. (2020). Efficient adsorbent derived from *Haloxylon recurvum* plant for the adsorption of acid brown dye: Kinetics, isotherm and thermodynamic optimization, *Surfaces and Interfaces*, 20, 100510. https://doi.org/ 10.1016/j.surfin.2020.100510
Isik Z., Bouchareb R., Arslan H., Özdemir S., Gonca S., Dizge N., Balakrishnan D. and Surya Prasad S.V. (2023). Green synthesis of iron oxide nanoparticles derived from water and methanol extract of *Centaurea solstitialis* leaves and tested for antimicrobial activity and dye decolorization capability, *Environmental Research*, **219**, 115072 https://doi.org/10.1016/j.envres.2022.11507
Kalia S., Samuchiwal S., Dalvi V. and Malik A. (2024). Exploring fungal-mediated solutions and its molecular mechanistic insights for textile dye decolorization, *Chemosphere*, **360**, 142370. https://doi.org/10.1016/j.chemosphere.2024.142370
Kapoor R.T., Danish M., Singh R.S., Rafatullah M. and HPS A.K. (2021). Exploiting microbial biomass in treating azo dyes contaminated wastewater: Mechanism of degradation and factors affecting microbial efficiency, *Journal of Water Process Engineering*, **43**, 102255. https://doi.org/10.1016/ j.jwpe.2021.102255
Khorramfar S., Mahmoodi N.M., Arami M. and Gharanjig K. (2010). Equilibrium and kinetic studies of the cationic dye removal capability of a novel biosorbent *Tamarindus indica* from textile wastewater, *Coloration Technology*, **126** (5), 261-268. https://doi:10.1111/j.1478-4408.2010.00256.x
Koyuncu H. and Kul A.R. (2020). Biosorption study for removal of methylene blue dye from aqueous solution using a novel activated carbon obtained from nonliving lichen (*Pseudevernia furfuracea* (L.) Zopf.). *Surfaces and Interfaces*, **19**, 100527. https://doi.org/10.1016/j.surfin.2020.100527
Lekhya K., Surendran R. and Elumalai L. (2025). Empowering a Nutritional Lifestyle through Soaked and Streamed Nuts Water Reuse using Novel RNN and NLP, Conference: 2024 International Conference on IT Innovation and Knowledge Discovery (ITIKD) https://doi.org/10.1109/ ITIKD63574.2025.11004716
Li H., Budarin V.L., Clark J.H., North M. and Wu X. (2022). Rapid and efficient adsorption of methylene blue dye from aqueous solution by hierarchically porous, activated starbons ®: Mechanism and porosity dependence, *Journal of Hazardous Materials*, **436**, 129174 https://doi.org/10.1016/j.jhazmat.2022.129174
Li X., Zhao Z., Xiao Q., He N., Kong J., Zhang D., Li R. and Shao, Q. (2023). Potential application of *Curtobacterium* sp. GX_31 for efficient biosorption of Cadmium: Isotherm and kinetic evaluation. *Environmental Technology & Innovation*, **30**, 103122. https://doi.org/10.1016/j.eti.2023.103122
Marungrueng K. and Pavasant P. (2006). Removal of basic dye (Astrazon Blue FGRL) using macroalga *Caulerpa lentillifera*, *Journal of Environmental Management*, **78** (3), 268–274. https://doi:10.1016/j.jenvman.2005.04.022
Maruthai S., Rajendran S., Selvanarayanan R. and Gowri S. (2025). Wastewater recycling integration with IoT sensor vision for realtime monitoring and transforming polluted ponds into clean ponds using HG-RNN, *Global NEST Journal*, **27** (4), 06758. https://doi.org/10.30955/gnj.06758
Mashkoor F., Nasar A., Inamuddin and Asiri A.M. (2018). Exploring the Reusability of Synthetically Contaminated Wastewater Containing Crystal Violet Dye using *Tectona grandis* Sawdust as a Very Low-Cost Adsorbent, *Scientific Reports*, **8** (1), 8314. https://doi:10.1038/s41598-018-26655-3
Mian A.H., Qayyum S., Zeb S., Fatima T., Jameel K. and Rehman B. (2024). Exploring indigenous fungal isolates for efficient dye degradation: A comprehensive study on sustainable bioremediation in the total environment, *Environmental Technology & Innovation*, **34**, 103615. https://doi.org/10.1016/j.eti.2024.103615
Mishra S., Cheng L. and Maiti A. (2021). The utilization of agro-biomass/byproducts for effective bio-removal of dyes from dyeing wastewater: A comprehensive review, *Journal of Environmental Chemical Engineering*, **9**, 104901 https://doi.org/10.1016/j.jece.2020.104901
Rai R. and Vijayakumar B.S. (2023). Myco-Remediation of Textile Dyes Via Biosorption by *Aspergillus tamarii* Isolated from Domestic Wastewater, *Water Air Soil Pollution*, **234**, 542. https://doi.org/10.1007/s11270-023-06535-x
Munagapati V.S., Wen H.-Y., Wen J.-C., Gutha Y., Tian Z., Reddy G.M. and Garcia J.R. (2020). Anionic congo red dye removal from aqueous medium using Turkey tail (*Trametes versicolor*) fungal biomass: adsorption kinetics, isotherms, thermodynamics, reusability, and characterization, *Journal of Dispersion Science and Technology*, **42** (12), 1–14. https://doi.org/10.1080/01932691.2020.1789468
Praveen S., Gokulan R., Pushpa T.B. and Jegan J. (2021). Techno-economic feasibility of biochar as biosorbent for basic dye sequestration, *Journal of the Indian Chemical Society*, **98** (8), 100107. https://doi:10.1016/j.jics.2021.100107
Rashdan H., Radwan E.K., Koryam A.A., El-Sayyed G. and Fathy R.M. (2023). Insights into promising basic red 18 dye removal and water disinfection utilizing novel sulfone biscompound-based chalcone derivative, *Journal of Water Process Engineering*, **54**, 104036. https://doi.org/10.1016/ j.jwpe.2023.104036
Rápó E., Posta K., Csavdári A., Vincze B.É. Mara G. Kovács G. Haddidi I. and Tonk S. (2020). Performance Comparison of *Eichhornia crassipes* and *Salvinia natans* on Azo-Dye (Eriochrome Black T) Phytoremediation, *Crystals*, **10** (7), 565. https://doi.org/10.3390/cryst10070565
Rybczyńska-Tkaczyk K., Korniłłowicz-Kowalska T., Szychowski K.A. and Gmiński J. (2020). Biotransformation and toxicity effect of monoanthraquinone dyes during *Bjerkandera adusta* CCBAS 930 cultures, *Ecotoxicology and Environmental Safety*, **191**, 110203 https://doi.org/10.1016/j.ecoenv.2020.110203
Samiyammal P., Kokila A., Pragasan L.A., Rajagopal R., Sathya R., Ragupathy S., Krishakumar M. and Minnam Reddy V.R. (2022). Adsorption of brilliant green dye onto activated carbon prepared from cashew nut shell by KOH activation:

Studies on equilibrium isotherm, *Environmental Research*, **212**, 113497. https://doi.org/10.1016/j.envres.2022.113497

Samuel M.S., John J. A., Ravikumar M., Raizada P., Wan Azelee N.I., Selvarajan E. and Selvasembian R. (2023). Recent progress on the remediation of dyes in wastewater using cellulose-based adsorbents, *Industrial Crops and Products*, **206**, 117590. https://doi.org/10.1016/j.indcrop.2023.117590

Selvanarayanan R., Rajendran S., Pappa C.K. and Thomas B. (2024). Wastewater recycling to enhance environmental quality using fuzzy embedded with RNN-IOT for sustainable coffee farming, *Global NEST Journal*, **26** (8), 06346. https://doi.org/10.30955/gnj.006346

Senthil Rathi B. and Senthil Kumar P. (2021). Application of adsorption process for effective removal of emerging contaminants from water and wastewater, *Environmental Pollution*, **280**, 116995. https://doi.org/10.1016/j.envpol.2021.116995

Shabir M., Yasin M., Hussain M., Shafiq I., Akhter P., Nizami A.-S., Jeon B.-H. and Park Y.-K. (2022). A review on recent advances in the treatment of dye-polluted wastewater. *Journal of Industrial and Engineering Chemistry*, **112**, 1-19. https://doi.org/10.1016/j.jiec.2022.05.013

Sillanpää, M., Mahvi A.H., Balarak D. and Khatibi A.D. (2023). Adsorption of Acid orange 7 dyes from aqueous solution using polypyrrole/nanosilica composite: Experimental and Modelling. *International Journal of Environmental Analytical Chemistry*, **103** (1), 212-229. https://doi.org/10.1080/03067319.2020.1855338

Singh G., Kumar V. and Dwivedi S.K. (2022). Comparative Investigation of Congo Red and Direct Blue-1 Adsorption on Mycosynthesized Iron Nanoparticle, *Journal of Cluster Science*, **33**, 1889-1905 https://doi.org/10.1007/s10876-021-02096-3

Sivarajasekar N., Baskar R., Ragu T., Sarika K., Preethi N. and Radhika T. (2017). Biosorption studies on waste cotton seed for cationic dyes sequestration: equilibrium and thermodynamics, *Applied Water Science*, **7**, 1987–1995. https://doi:10.1007/s13201-016-0379-2

Slimani R., El Ouahabi I., Abidi F., El Haddad M., Regti A., Laamari M.R., El Antri S., Lazar S. (2014). Calcined eggshells as a new biosorbent to remove basic dye from aqueous solutions: Thermodynamics, kinetics, isotherms and error analysis, *Journal of the Taiwan Institute of Chemical* Engineers. **45** (4), 1578-1587. https://doi.org/10.1016/j.jtice.2013.10.00

Sravan J.S., Matsakas L. and Omprakash Sarkar O. (2024). Advances in Biological Wastewater Treatment Processes: Focus on Low-Carbon Energy and Resource Recovery in Biorefinery Context, *Bioengineering*, **11** (3), 281. https://doi.org/10.3390/bioengineering11030281

Sudarshan S., Harikrishnan S., Bhuvaneswari G.R., Alamelu V., Aanand S., Aruliah Rajasekar A. and Govarthanan M. (2022). Impact of textile dyes on human health and bioremediation of textile industry effluent using microorganisms: current status and future prospects, *Journal of Applied Microbiology*, **134** (2), 1-23. https://doi.org/10.1093/jambio/lxac064

Syafiuddin A. and Fulazzaky M.A. (2021). Decolorization kinetics and mass transfer mechanisms of Remazol Brilliant Blue R dye mediated by different fungi. *Biotechnology Reports*, **29**, e00573. https://doi.org/10.1016/j.btre.2020.e00573

Tokay Yılmaz F.G., Tekin G., Ersöz G. and Atalay S. (2023). Reclamation of real textile wastewater by sequential advanced oxidation and adsorption processes using corn-cob based materials, *Environmental Pollution*, **335**, 122196. https://doi.org/10.1016/j.envpol.2023.122196

Toptas A., Demierege S., Mavioglu Ayan E. and Yanik J. (2014). Spent Mushroom Compost as Biosorbent for Dye Biosorption, *CLEAN - Soil, Air, Water*, **42** (12), 1721–1728. https://doi:10.1002/clen.201300657

Torres-Farradá G., Thijs S., Rineau F., Guerra G. and Vangronsveld J. (2024). White Rot Fungi as Tools for the Bioremediation of Xenobiotics: A Review, *Journal of Fungi*, **10** (3), 167. https://doi.org/10.3390/jof10030167

Tran T.-K., Huynh L., Nguyen H.-L., Nguyen M.-K., Lin C., Hoang T.-D., Hung N.T.Q., Nguyen X.H., Chang S.W. and Nguyen D.D. (2024). Applications of engineered biochar in remediation of heavy metal(loid)s pollution from wastewater: Current perspectives toward sustainable development goals, *Science of The Total Environment*, **926**, 171859. https://doi.org/10.1016/j.scitotenv.2024.171859

Tukaram bai, M., Shaik O., Kavitha J., Hemanth Varma, M.S. and Chittibabu N. (2020). Biosorption of eosin yellow dye from aqueous solution using *sugarcane bagasse*: Equillibrium, kinetics and thermodynamics. *Materials Today: Proceedings*, **26**, (2), 842-849. https://doi.org/10.1016/j.matpr.2020.01.051

Verma A., Kumar S. and Kumar S. (2017). Statistical modeling, equilibrium and kinetic studies of cadmium ions biosorption from aqueous solution using *S. filipendula*, *Journal of Environmental Chemical Engineering*, **5** (3), 2290-2304. https://doi.org/10.1016/j.jece.2017.03.04

Wang Y., Jiang, L., Shang H., Li Q. and Zhou W. (2020). Treatment of azo dye wastewater by the self-flocculating marine bacterium *Aliiglaciecola lipolytica*. *Environmental Technology & Innovation*, **19**, 100810. https://doi.org/10.1016/j.eti.2020.100810

Wen H., Cheng D., Chen Y., Wenhui Yue W. and Zhang Z. (2024). Review on ultrasonic technology enhanced biological treatment of wastewater, *Science of The Total Environment*, **925**, 171260. https://doi.org/10.1016/j.scitotenv.2024.171260

Yaacoobi F.E., Sekkouri C., Ennaciri K., Rabichi I., Izghri Z., Baçaoui A. and Yaacoubi, A. (2024). Synthesis of composites from activated carbon based on olive stones and sodium alginate for the removal of methylene blue. *International Journal of Biological Macromolecules*, **254** (3), 127706. https://doi.org/10.1016/j.ijbiomac.2023.127706

Yadav A. and Dindorkar S.S. (2022). Adsorption behaviour of hexagonal boron nitride nanosheets towards cationic, anionic and neutral dyes: Insights from first principle studies, *Colloids and Surfaces A: Physicochemical and Engineering Aspects*, **640** (5), 128509 https://doi.org/10.1016/j.colsurfa.2022.128509

Yang Y., Jin D., Wang G., Liu D., Jia X. and Zhao Y. (2011). Biosorption of Acid Blue 25 by unmodified and CPC-modified biomass of *Penicillium* YW01: Kinetic study, equilibrium isotherm and FTIR analysis. *Colloids and Surfaces B: Biointerfaces*, 88 (1), 521–526. https://doi.org/10.1016/j.colsurfb.2011.07.047